



TECHNICAL ARTICLE

Effect of Brazing Clearance on the Microstructure and Mechanical Properties of TC4/TC4 Joints Brazed in Vacuum with Ti–Zr–Ni Filler Metal

Min Liang, Youqiong Qin, Danfeng Zhang, and Feng Zhao

Submitted: 16 May 2022 / Revised: 27 June 2022 / Accepted: 10 July 2022 / Published online: 9 September 2022

Vacuum brazing was used to join TC4 titanium alloy with self-designed and non-copper Ti–38Zr–24Ni (wt.%) filler metal. Variable brazing clearances were chosen to study their effect on the microstructural evolution and mechanical properties of the joints. The brazed joint with narrow brazing clearance only contained two reaction zones: the diffusion zone (α -Ti and (Ti, Zr)₂Ni eutectoid structures and remained based metal) and the interface zone (α -Ti and (Ti,Zr)₂Ni). However, the brazed joint with large brazing clearance had another reaction zone in the middle of the joint: the center zone (big block brittle (Ti,Zr)₂Ni IMCs and some tiny phases: α -Ti and (Ti,Zr)₂Ni eutectoid transformation phase). The width of center zone increased with the increase of the brazing clearance. The maximum shear strength of the brazed joint reached 872 MPa when brazing clearance was 0 μ m. The brittleness of IMCs in center zone caused the low strength of the joint. Quasi-cleavage fracture occurred in the narrow brazing clearance (0 μ m), while mixed quasi-cleavage and cleavage fractures occurred in the large brazing clearance (50–200 μ m).

Keywords TC4, brazing clearance, microstructural evolution, strength, vacuum brazing

1. Introduction

Since the middle of the last century, titanium alloys have been regarded as the third metal or the future metal because of their excellent properties, such as low density, high specific strength, good corrosion resistance and good process performance. They are contributed significantly to the development of aerospace shipping and other industrial fields. Among them, TC4 is the most widely used titanium alloy (Ref 1). Fusion welding and solid state welding can be used to join titanium alloys. However, to some complex components, brazing, especially vacuum brazing, is the only method to join them due to its advantages of low brazing temperature, slight deformation of the specimens and being free from impurity gas contamination (Ref 2–4).

During the process of brazing, many brazing parameters will affect the quality of the brazed joint, such as type of filler metal, brazing temperature, holding time, brazing clearance and shielding gas atmosphere. Because of the chemical reactivity of the titanium alloys, the brazing is usually processed in a vacuum.

For type of filler metal, four commonly filler metals (silver-based, aluminum-based, palladium-based and titanium-based)

have been used to braze titanium alloys (Ref 5–8). However, the low using temperature limits the application of aluminum-based and silver-based filler metals. Therefore, Ti-based (or Ti–Zr-based) filler metals are the popular filler metals to join titanium alloys not only because of its good compatibility with titanium alloys but also due to the high strength, good thermal resistance and corrosion resistance of the brazed joint close to the based metal.

The holding time and brazing temperature are the other two important parameters of influence the quality of brazed joint. Ultrahigh brazing temperature leads to a large of intermetallics which raises the brittleness of the joint. Botstein et al. (Ref 9) reported that γ -(Ti,Zr)₂Cu and λ -Cu₂(Ti,Zr) intermetallic existed in middle of brazing seam during the brazing of TC4 with Ti–25Zr–50Cu (wt.%). The brittleness of the brazed joint deteriorated the mechanical properties. Moreover, if the brazing temperature is over the β transus temperature, the strength of the based metal would deteriorate (Ref 10, 11). However, if the brazing temperature is so low, the reaction is not sufficient which leads to defective joint. Similarly, suitable holding time is beneficial to obtain high-quality joint (Ref 12).

Another brazing parameter to affect the quality is brazing clearance. Common brazing clearances shouldn't exceed 0.15 mm. The molten filler metal flows into the brazing clearance due to capillary action and reacts with the based metal and then forms the joint. If the brazing clearance is very large, the capillary action is weak which may influence the quality of the brazed joint. Some researchers adopted many methods to solve this problem. Radzievskii et al. (Ref 13) added powders in the brazing gap to increase the capillary action. Moreover, even with narrow brazing clearance, different brazing clearances may lead to variable microstructure and strength of the brazed joint. Chen et al. (Ref 14) studied the vacuum brazing of 316L stainless steel by BNi-2 nickel-based filler metal. It was found that when the brazing clearance was under 40 μ m, the

Min Liang, Youqiong Qin, Danfeng Zhang, and Feng Zhao, School of Material Engineering, Shanghai University of Engineering Science, Shanghai 201620, People's Republic of China. Contact e-mail: yqqin@163.com.

microstructure of the joint was ductile solid solution and the strength of the joint was high but large brazing clearance (such as 80 μ m) led to low strength. Kavishe et al. (Ref 15) reported during the brazing steel with Cu, the tensile strength increased with the decreased brazing clearance but the fracture toughness decreased at a very low level with the decreased brazing clearance. Baumgartner et al. (Ref 16) reported that regardless of the brazing process used, there is a tendency in the area of

the brazing gap width for the number and size of defects to increase with increasing gap size, which can negatively affect fatigue strength depending on the damage behavior.

During the brazing of the titanium alloy with Ti- or Ti(Zr)-based filler metal, some melting point depressants (MPDs) (such as Zr, Cu, Ni, Be) added in the filler metal would generate brittle intermetallic compounds in the joint and decreased the strength of the joint (Ref 17). It is very important to choose suitable brazing parameters to control the amount of the IMCs and obtain high quality of the brazed joint. However, few researchers have reported the choosing brazing clearance during brazing titanium alloy with Ti- or Ti(Zr)-based filler metal. In this experiment, a Ti-Zr-based filler metal containing no Cu (Ti-38Zr-24Ni, wt.%) was self-made and the effect of brazing clearance (0 μ m (natural gap), 50, 100 and 200 μ m) on the microstructure and strength of the TC4/TC4 joint were discussed. Simultaneously, the microstructure transformation

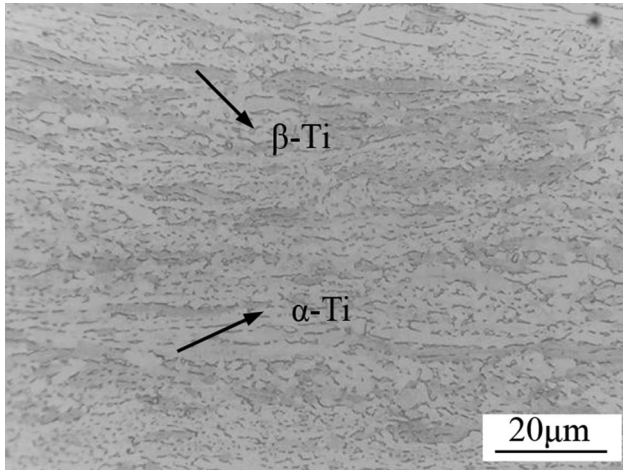


Fig. 1 Microstructure of TC4

Table 1 The brazing parameters in the experiment

	Brazing temperature, °C	Holding time, min	Brazing clearance (Theoretically), μ m
No.1	930	10	0
No.2	930	10	50
No.3	930	10	100
No.4	930	10	200

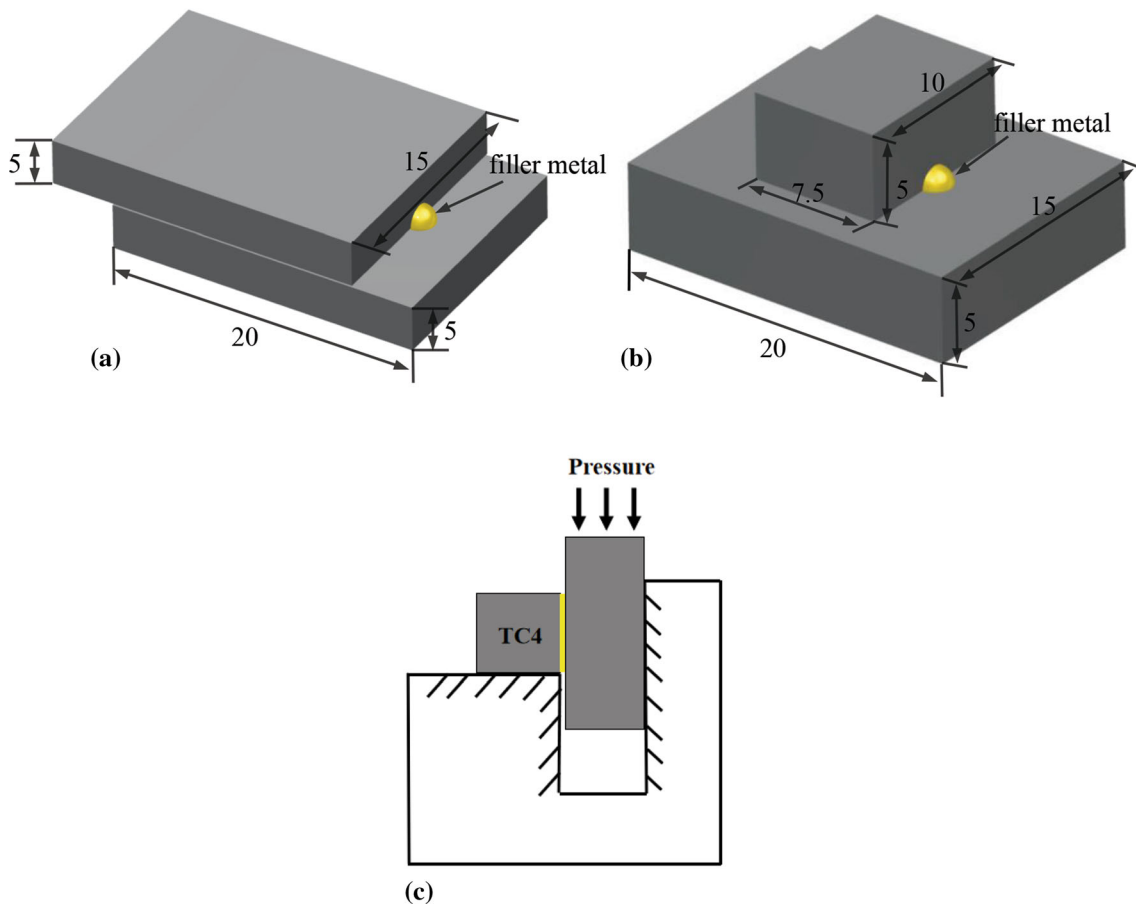


Fig. 2 Schematic diagram of brazed specimen assembly (length unit: mm): (a) microstructure analysis specimen; (b) shear strength analysis specimen. (c) sectional view of shear strength test

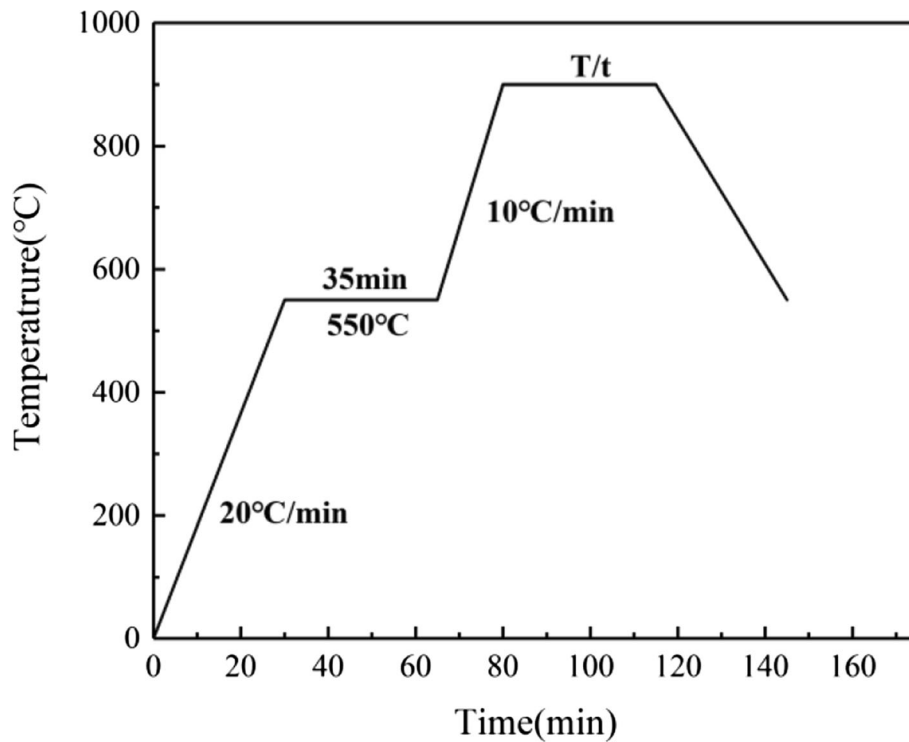


Fig. 3 Time-temperature heating curve of brazing process

and fracture pattern of the joints were also studied. The studying is apt to provide the reference for the choice of brazing titanium alloy.

2. Experimental Procedures

TC4 (Ti-6Al-4 V, wt.%) titanium alloy was employed as based metal. Its microstructure is α -Ti phases (blocky) and around β -Ti phases (Fig. 1). Before brazing, the TC4 based metal needed to be rolled. The filler metal was self-designed and prepared. 99.99% pure Ti, Zr and Ni blocks were weighed by mass ratio and then melted them three times by an electric arc furnace equipped with magnetic stirring. A homogeneous alloy ingot was obtained, and its chemical composition was Ti-38Zr-24Ni (wt.%). The melting region of the filler metal was about 847–869 °C obtained by differential scanning calorimetry (DSC) with heating speed (20 °C/min).

Before brazing, the TC4 based metal was prepared into the size of $10 \times 7.5 \times 5$ and $20 \times 15 \times 5$ mm by wire cutting machine, and all the specimens of based metal and pieces of the filler metal were ground by abrasive papers from 80 to 1000# and then cleaned in the acetone for 15 min and dried by air blowing. TC4 were overlapped for microstructural specimen and mechanical property specimen. 50, 100 and 200 μm Ti foils were used to control the brazing clearance. Three small Ti foils (about 1×1 mm) were put in the brazed joint. The filler metal was placed in the corner of the brazing clearance. Through calculating the volume of the different brazing gaps (V) and the density of the filler metal (ρ), the volume was obtained by $V = L(\text{length}) \times W(\text{width}) \times H(\text{height})$. A suitable weight

($m = \rho V$) of the filler metal species was adopted. Figure 2 gives the installation schematic diagram.

In this experiment, the brazing clearance varied from 0 to 200 μm . The samples are brazed using a multifunctional scientific and educational vacuum furnace (model: WHQ-200). The brazing parameters are shown in Table 1. The time vs temperature heating curve is shown in Fig. 3. After brazing, the metallographic samples were ground, polished and etched using 3 ml HF + 36mlHNO₃ + 100mlH₂O. Scanning electron microscope (SEM) (model: S-3400 N) or optical microscopy (OM) (model: VHX-5000) was adopted to analyze the microstructure and fracture surface. The composition of phases was determined by an energy-dispersive spectrometer (EDS) (model: S-3400 N). The compressing shear test was used to obtain the shear strength and the compressing rate was 1 mm/min. The average shear strength was from three samples in every case. The melting point was obtained by DSC differential scanning calorimetry. The phases in the fracture surface were investigated by X Perp PRO x-ray diffraction (XRD). Cu K α was selected as the source of X-rays with a scan range of 0–80° and a speed of 8°/min.

3. Results

3.1 Microstructure of the Brazed Joints

With different brazing clearances, the microstructure of the brazed joints was changed. The OM images of the brazed joints are shown in Fig. 4. All the brazed joints had no defects. With narrow brazing clearances, two reaction zones existed in the

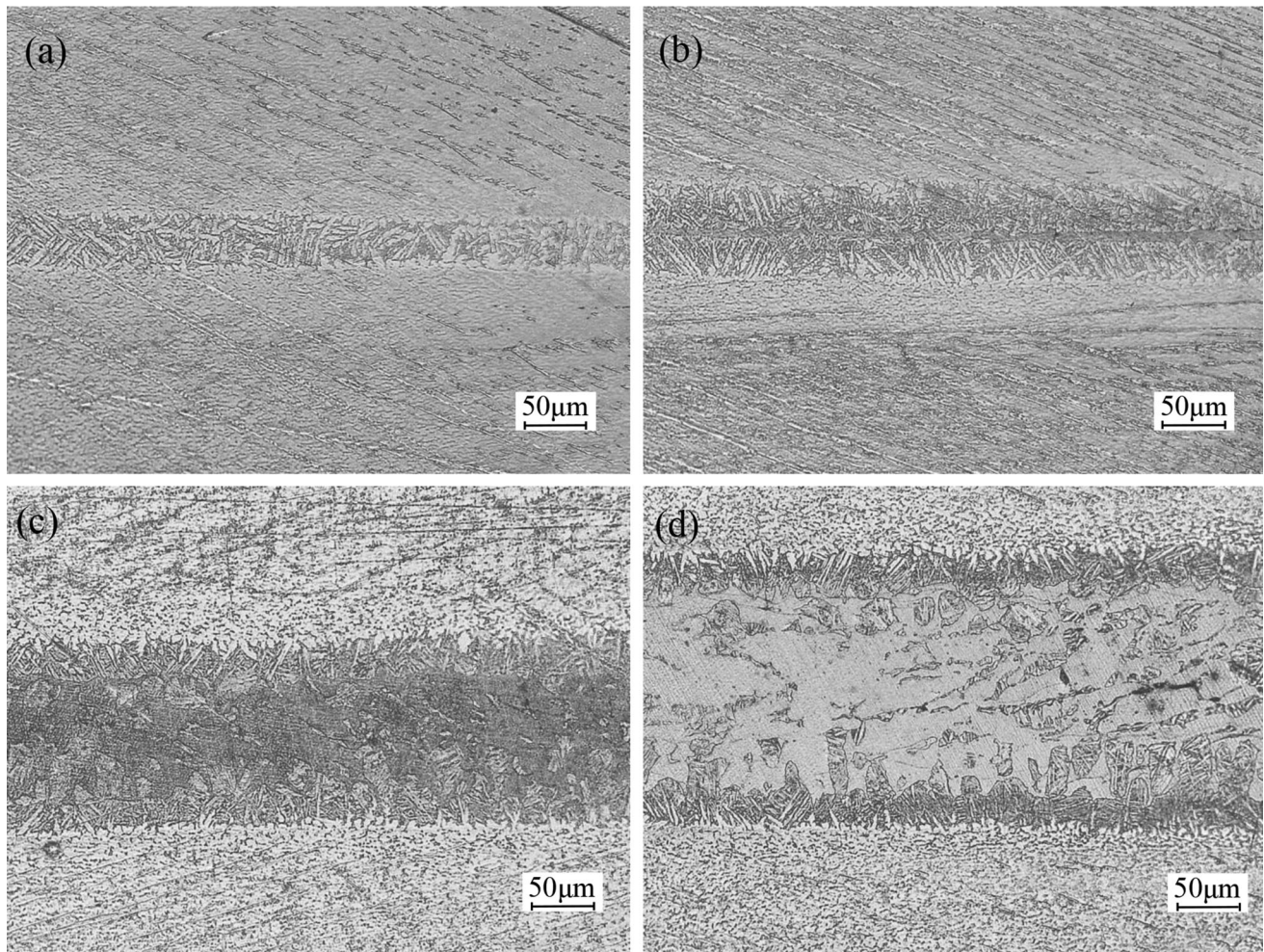


Fig. 4 Microstructure of the brazed joints for different brazing clearances: (a) 0 μm ; (b) 50 μm ; (c) 100 μm ; (d) 200 μm

brazed joint but three reaction zones existed with large brazing clearances. (The detailed analysis of microstructure will be discussed in the following.) The actual brazing clearances were larger than that proposed theoretically.

To clearly analyze the microstructure, SEM and EDS analysis of the typical interface microstructure of the brazed joint with 0 and 100 μm brazing clearance is shown in Fig. 5 and Table 2. From Fig. 5(a) and (b), when the brazing clearance was narrow, the width of the brazing clearance was about 40 μm , which was primarily wider than the predetermined level (0 μm). There existed two reaction zones in the brazed joint: diffusion zone and interface zone, respectively (marked as I, II). Different to the narrow brazing clearance, the brazed joints with large brazing clearance had three distinctive reaction zones: diffusion zone, interface zone and center zone, respectively (marked as I, II and III), as shown in Fig. 5(c) and (d).

As shown in Fig. 5(b) (No.1), zone I differed slightly from zone II. Zone I contained irregular and mesh-like black phase (point E_1) and white phase (point E_2), but zone II contained regular black phase (point F_1) and white phase (point F_2). The black phase (point E_1) was mainly composed of Ti. It was near the based metal. So, it was α -Ti of original based metal. The white phase (point E_2) was mainly constituted by 37.31at.% Ti, 29.28at.% Zr and 26.38at.% Ni. The atomic percentage of

(Ti + Zr) and Ni was about 2:1. Therefore, the white phase was $(\text{Ti,Zr})_2\text{Ni}$ intermetallic compound, corresponding to the result in references (Ref 18-20). During the brazing process, some Ni and Zr elements diffused into the TC4 based metal at first and the eutectoid transformation occurred in the following. So, zone I was α -Ti + $(\text{Ti,Zr})_2\text{Ni}$.

For Zone II (No.1), the chemical composition of the black phase (F_1) and the white phase (F_2) was similar to the E_1 and E_2 , respectively. Nevertheless, the black and white phases exhibited the lamellar structure. During brazing, in addition to the diffusion of Zr and Ni atoms to the based metal, Ti from the based metal melted into the molten filler metal. The brazing process can be regarded as a transient liquid phase (TLP) bonding. All the molten filler metal transformed the precipitated phase (β -Ti) due to the diffusion and dissolution existed between the based metal and filler metal during brazing. In the following decreasing of the brazing temperature, the precipitated phase (β -Ti) transformed to the laminar structure with black and white by eutectoid transformation (β -Ti \rightarrow α -Ti + $(\text{Ti,Zr})_2\text{Ni}$)_{eutectoid}. Therefore, zone II (No.1) contained the α -Ti + $(\text{Ti,Zr})_2\text{Ni}$ lamellar structure.

For No.3 specimen, the microstructure and element content of zone I (No.3) and zone II(No.3) were similar to zone I (No.1) and zone II (No.1), respectively, as shown in Fig. 5(c) and

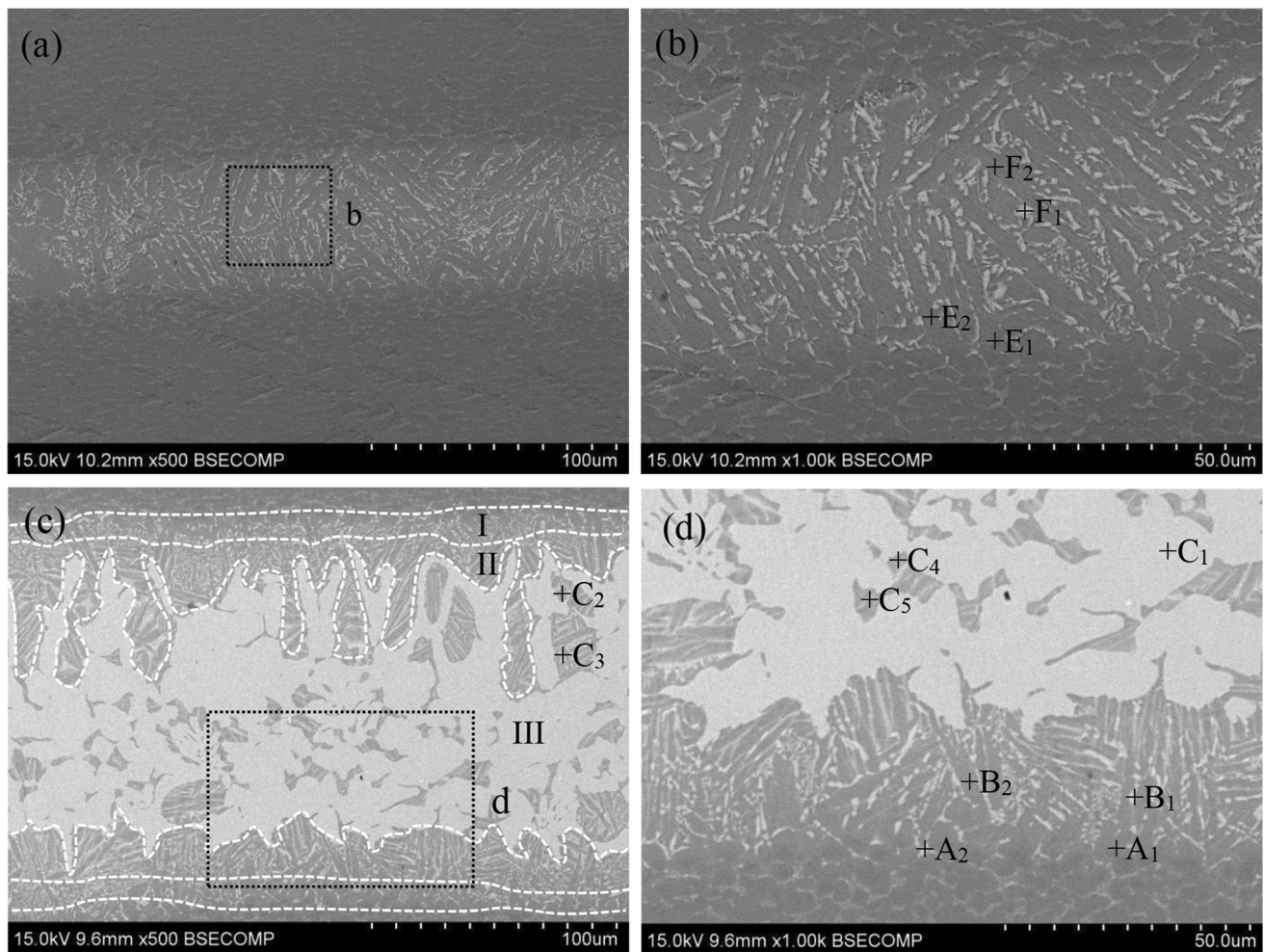


Fig. 5 Microstructures and major element content distribution of brazed joint: (a) microstructure of the brazed joints at 0 μm brazing clearance, (b) high-magnification images in (a), (c) microstructure of the brazed joints at 100 μm brazing clearance, (d) high-magnification images of zone I and zone II + III

Table 2 Average chemical composition (at.%) analysis and possible phases in Fig. 5(a) (No.1) and Fig. 5(c) (No.3)

Zone	Position	Ti	Zr	Ni	V	Al	Possible phase
I(No.1)	E1	79.41	2.24	1.76	4.55	12.04	α -Ti (high Ti concentration)
I(No.1)	E2	37.31	29.28	26.38	1.02	6.01	$(\text{Ti}, \text{Zr})_2\text{Ni}$
II(No.1)	F1	71.81	13.27	9.38	2.95	2.59	α -Ti
II(No.1)	F2	36.01	30.87	28.09	1.92	3.11	$(\text{Ti}, \text{Zr})_2\text{Ni}$
I(No.3)	A ₁	86.31	1.98	1.33	2.24	8.14	α -Ti (high Ti concentration)
I(No.3)	A ₂	35.65	25.20	27.85	4.27	7.03	$(\text{Ti}, \text{Zr})_2\text{Ni}$
II(No.3)	B ₁	75.57	11.15	0.92	1.12	11.24	α -Ti
II(No.3)	B ₂	30.45	32.26	29.50	4.35	3.44	$(\text{Ti}, \text{Zr})_2\text{Ni}$
III(No.3)	C ₁	32.53	30.56	30.13	3.56	3.22	$(\text{Ti}, \text{Zr})_2\text{Ni}$
III(No.3)	C ₂	75.68	11.52	9.45	1.82	1.53	α -Ti
III(No.3)	C ₃	30.65	32.26	30.65	3.30	3.14	$(\text{Ti}, \text{Zr})_2\text{Ni}$
III(No.3)	C ₄	74.53	11.53	11.48	1.62	0.84	α -Ti
III(No.3)	C ₅	30.47	32.45	30.71	3.34	3.03	$(\text{Ti}, \text{Zr})_2\text{Ni}$

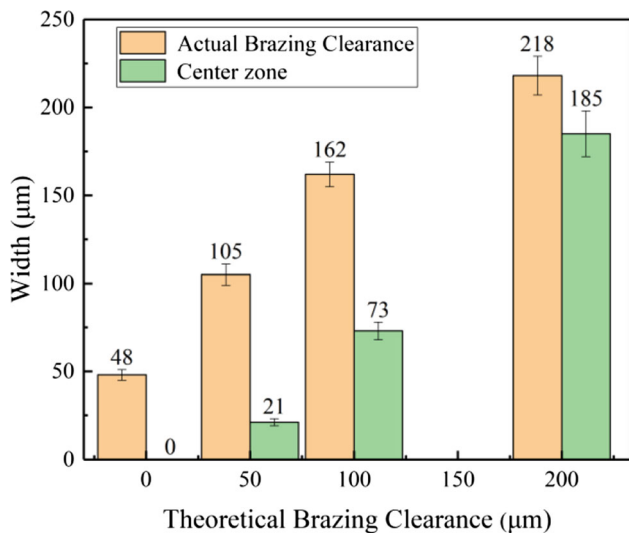


Fig. 6 Effect of brazing clearance on width of the brazed joints

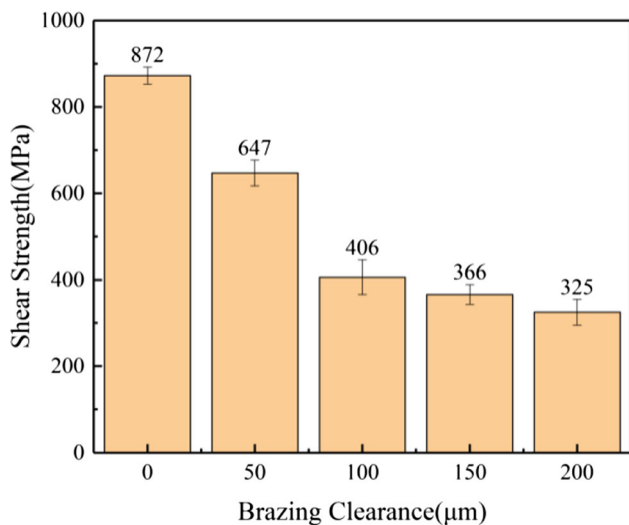


Fig. 7 Effect of brazing clearance on shear strength of the brazed joints

Table 2. Therefore, zone I (No.3) was α -Ti + (Ti,Zr)₂Ni, and zone II (No.3) was the α -Ti + (Ti,Zr)₂Ni lamellar structure.

Different from the joint in No.1, the brazed joint with large brazing clearance existed another zone: zone III (such as No.3). Zone III (No.3) contained the big block white phase and the lamellar structure with black and white. The big block white phase (point C₁) consisted of 32.53at.% Ti, 30.56at.% Zr and 30.13at.% Ni. According to the Ti(Zr)-Ni phase diagram, it was (Ti, Zr)₂Ni. Two sizes of lamellar structure (the big size (C₂ + C₃) and the small size (C₄ + C₅)) were obviously shown in the central zone. The black phase (points C₂ and C₄) mainly

contained Ti and Zr. It was α -Ti. The white phase (point C₃ and C₅) mainly contained Ti, Zr and Ni; it was similar to point B₂, so it was (Ti, Zr)₂Ni. With large brazing clearance, the diffusion distance was longer than that with narrow brazing clearance. Therefore, a lot of Zr and Ni remained in the middle of brazing seam which caused the existing of liquid remained filler metal in the middle of brazing seam. During the cooling process, β -Ti was also precipitated from the melted filler metal in the middle of the brazing clearance due to the non-equilibrium solidification, which formed the big sized lamellar structure ($L \rightarrow \beta$ -Ti + L)_{hypo-eutectic}. Then when the temperature cooled to the eutectic temperature, the eutectic transformation occurred ($L \rightarrow \beta$ -Ti + (Ti, Zr)₂Ni)_{eutectic}. The big block white phase (Ti, Zr)₂Ni formed. Finally, both of the precipitated β -Ti and eutectic transformation β -Ti transformed to the lamellar structure with black and white by eutectoid transformation (β -Ti \rightarrow α -Ti + (Ti, Zr)₂Ni)_{eutectoid}. The size of the precipitated phase was usually bigger than the eutectic transformation phase due to the longer crystallization time.

From the above, when the brazing clearance was narrow, the brazed joint contained two reaction zones. No intermetallic compound existed in the middle of joint. Increasing the brazing clearance, low melting point filler metal remained in the middle of brazing seam which formed central zone. With the increased brazing clearance, the widths of the whole brazing seam and the central zone increased, as shown in Fig. 6. This is because in other brazing condition invariable situation, the diffusion distance of Ni and Zr from the filler metal into based metal and the dissolution distance of Ti from the based metal into filler metal become larger with wider brazing clearance. Both of the reasons caused more proportion of Ni in the middle of the filler metal. According to the solidification theory of hypoeutectic alloys and Ti(Zr)-Ni phase diagram, when the temperature dropped, β -Ti solid solution phases formed near the based metal since it was easier to nucleate on the surface of the solid phase. Meanwhile, β -Ti precipitated phase also formed at Ti-rich region in the liquid alloy. As the temperature continued to drop, the dimension of β -Ti increased. Meanwhile, the residual liquid phase had a high and basically Ni content because of the consumption of Ti. Finally, eutectic transformation occurred which led to form center zone. Therefore, the center zone contained amount of Ti(Zr)₂Ni intermetallic compound.

3.2 Mechanical Properties of the Brazed Joints

With different brazing clearances, the average shear strength of the brazed joints varied, as shown in Fig. 7. Increasing the brazing clearance, the average shear strength of the brazed joints decreased. The maximum shear strength of the brazed joints was 872 MPa at the brazing clearance of 0 μ m (theoretically). That is to say, narrow brazing clearance was beneficial to obtain high strength. In practical condition, the real brazing clearance should be narrow as far as possible. From the result of the microstructure, when the brazing clearance was narrow, there was no or little Ti(Zr)₂Ni intermetallic compound. Since (Ti,Zr)₂Ni intermetallic compound was a brittle phase, the crack was easy to produce and extend in it. Therefore, high shear strength of the brazed joints was obtained with narrow

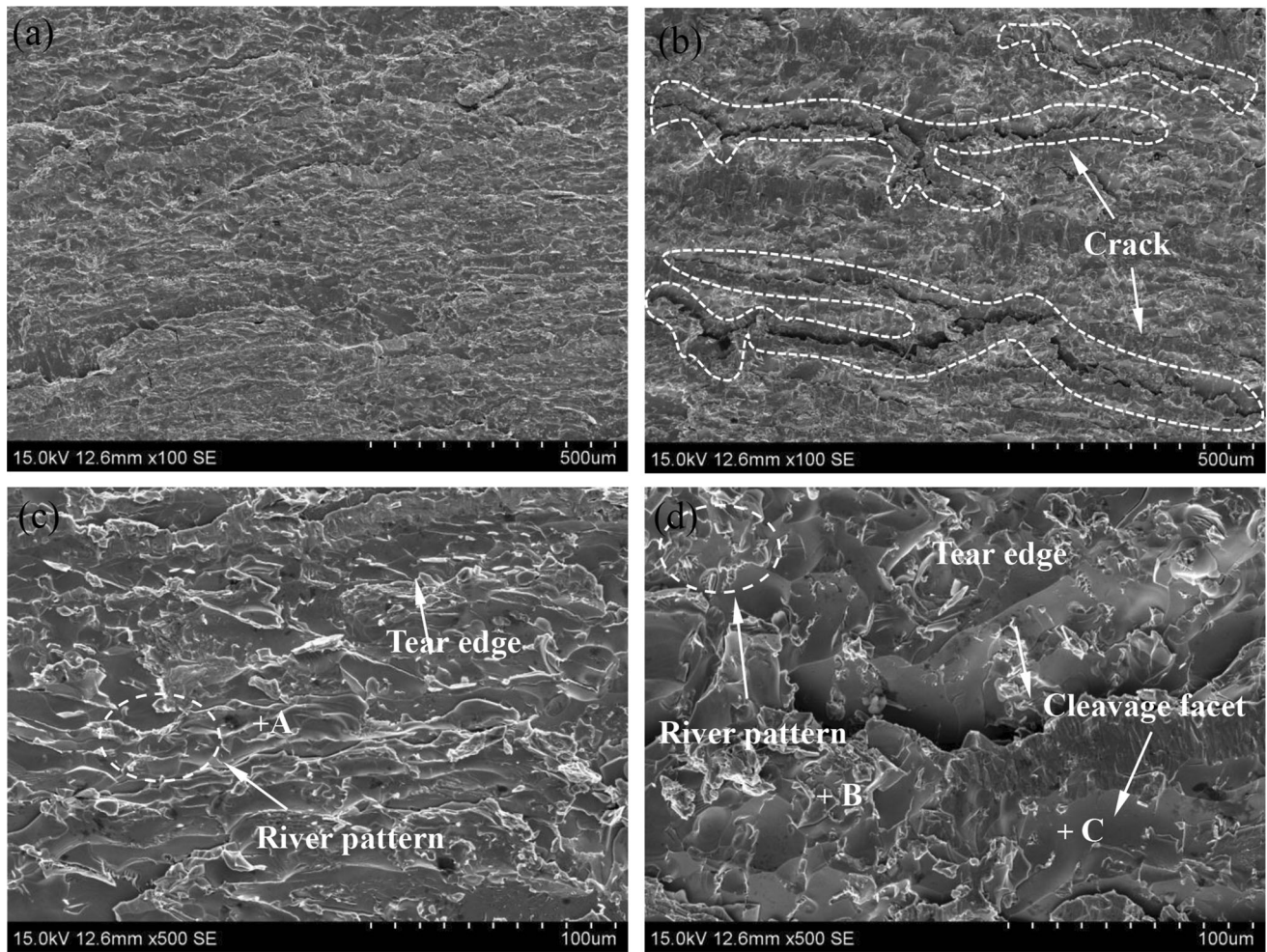


Fig. 8 The fracture morphology of the brazed joints under different brazing conditions after room temperature shear strength test: (a) and (c) 0 μm ; (b) and (d) 100 μm

Table 3 The chemical compositions (at.%) of different positions in Fig. 8

	Ti	Zr	Ni	V	Al	Possible phase
A	72.54	11.12	9.85	1.76	4.73	eutectoid phases
B	79.23	10.28	6.43	1.82	2.24	eutectoid phases
C	34.25	30.54	31.78	1.57	1.86	(Ti, Zr) ₂ Ni

clearance. However, great brittle Ti(Zr)₂Ni intermetallic compounds in the middle of brazing seam led to low shear strength.

3.3 Fracture Analysis of the TC4-TC4 Brazed Joint

Figure 8 reveals the fracture morphology of the brazed joints at the brazing clearance of 0 and 100 μm after tensile shear testing, and average chemical composition of the marked points in Fig. 8 is listed in Table 3. Through the analysis of typical fracture morphology under high-magnification images,

the fracture mode at the brazing clearance of 0 μm was quasi-cleavage fracture (Fig. 8c), while the fracture mode at the brazing clearance of 100 μm mixed the cleavage and quasi-cleavage fracture (Fig. 8d). Locations A and B were composed of a fine river pattern, tear ridges or step lines. The fracture pattern was quasi-cleavage fracture. Based on the microstructure of the brazed joint and average chemical composition of locations A and B in Table 3, locations A and B were the eutectoid structure (α -Ti and (Ti,Zr)₂Ni). Location C featured cleavage planes and steps. The fracture pattern was typical cleavage fracture. Its atomic percentage of (Ti + Zr) and Ni was about 2:1. So, Location C was brittle (Ti,Zr)₂Ni intermetallic compounds. Moreover, from the XRD results (Fig. 9), the fracture surface with the brazing clearance of 0 μm mainly contained α -Ti and a little of (Ti,Zr)₂Ni but the fracture surface with the brazing clearance of 100 μm not only contained α -Ti but also great of (Ti,Zr)₂Ni. Therefore, the fracture with the brazing clearance of 0 μm occurred in the interface zone but the fracture with the brazing clearance of 100 μm occurred in the center zone. This was the reason why high value shear strength

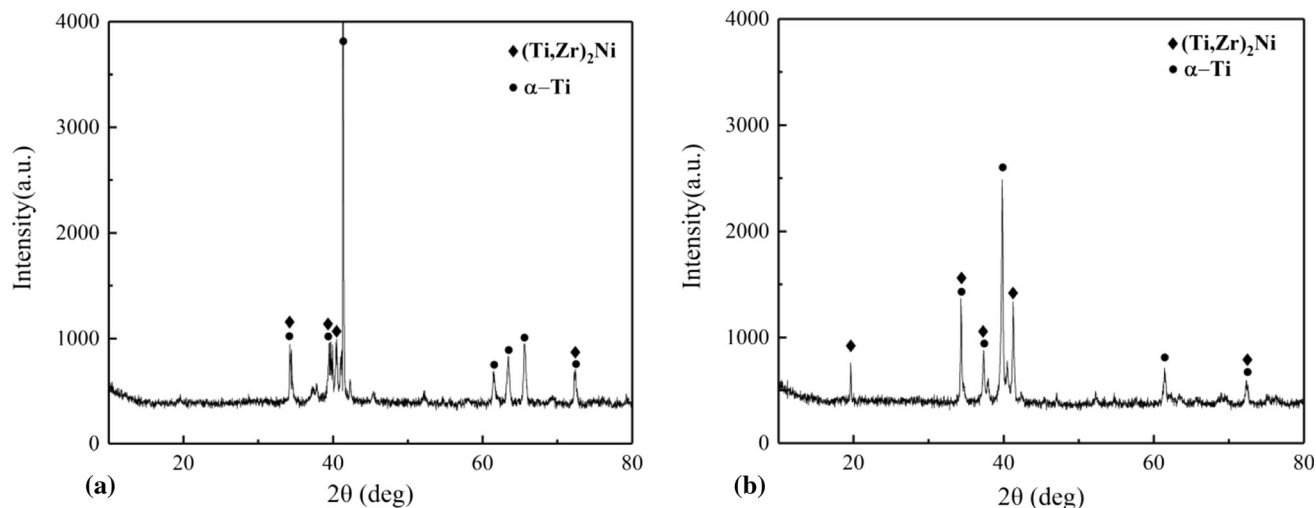


Fig. 9 The XRD analysis of the fracture surface under different brazing conditions: (a):0 μm ; (b):100 μm

of the joints was obtained with brazing clearance of 0 μm . Compared to the fracture morphology between 0 and 100 μm , more areas with cleavage fracture existed at wider brazing clearance. This was identical to many previous research surveys (Ref 21, 22).

4. Discussion

Figure 10 displays the Ti(Zr)–Ni phase diagram (Ref 23) and a conceptual interface evolution model for the brazed joint by ternary filler metal. Figure 10(a) represents the Ti(Zr)–Ni phase diagram; the two blue dashed lines represent two types of different brazing clearances. The study of the nucleation and growth mechanism of the reactive phase in the brazing seam is based on this phase diagram. Figure 10(b, c and e) shows the conceptual microstructural evolution. They contain atomic diffusion characteristics and the formation of reaction phases.

The first stage: the melting of filler metal. The based metal and filler metal contact with each other from room temperature to the melting point of the filler metal. As the filler metal turns into the molten state, the filler metal quickly fills in the brazing clearance (Fig. 10b).

The second stage: diffusion and dissolution. Due to the concentration difference, some Ti atoms in TC4 partially dissolve into the liquid alloy, while Ni and Zr atoms diffuse from the molten alloy into the based metal (Fig. 10c).

The last stage: freezing of reaction phases. During the holding time at brazing temperature or the early cooling process after reaching brazing temperature, β -Ti solid solution nucleates and grows at the TC4/filler metal interface. Meanwhile, precipitated β -Ti may be formed in the central brazing seam

due to nonequilibrium solidification. Solid β -Ti thickens both at TC4/filler metal interface and in the center of brazing seam. If the brazing clearance is very narrow (such as 0 μm), solid β -Ti quickly fills full of the brazing seam. The brazing process is similar to TLP bonding. The brazed joint contains only two reaction zones at last (Fig. 10e). If the brazing clearance is large, the diffusion and dissolution between based metal and filler metal is not adequate. The remained filler metal in the middle of brazing seam is liquid. As the temperature declines to the eutectic temperature, the eutectic reaction of $L \rightarrow \{\beta\text{-Ti} + (\text{Ti}, \text{Zr})_2\text{Ni}\}_{\text{eutectic}}$ occurs in the residual liquid. At that time, the brazed joint with large brazing clearance contains three reaction zones. The central brazing seam consists in big block β -Ti (from precipitated first), tiny β -Ti (from eutectic reaction) and $(\text{Ti}, \text{Zr})_2\text{Ni}$ (Fig. 10d). Finally, with the narrow brazing clearance or with the large clearance, when the temperature continues to cool down to the eutectoid point, the eutectoid reaction of $\beta\text{-Ti} \rightarrow \{\alpha\text{-Ti} + (\text{Ti}, \text{Zr})_2\text{Ni}\}_{\text{eutectoid}}$ occurs according to Ti(Zr)–Ni phase diagram.

From the above, the brazed joint with narrow brazing clearance contains only two reaction zones at room temperature: Diffusion zone contains original α -Ti, eutectoid transformation α -Ti and $(\text{Ti}, \text{Zr})_2\text{Ni}$. Interface zone contains lamellar $(\text{Ti}, \text{Zr})_2\text{Ni}$ and α -Ti by eutectoid transformation (the blue line ② (Range: A–B) shown in Fig. 10a). Differently, the brazed joint with large brazing clearance contains only two reaction zones at room temperature: The diffusion zone and interface zone are similar to that of narrow brazing clearance, but the center zone contains big block lamellar $(\text{Ti}, \text{Zr})_2\text{Ni}$ and α -Ti, tiny lamellar $(\text{Ti}, \text{Zr})_2\text{Ni}$ and α -Ti, together with some $(\text{Ti}, \text{Zr})_2\text{Ni}$ by eutectic transformation (the blue line ① (Range: B–C) shown in Fig. 10(a)).

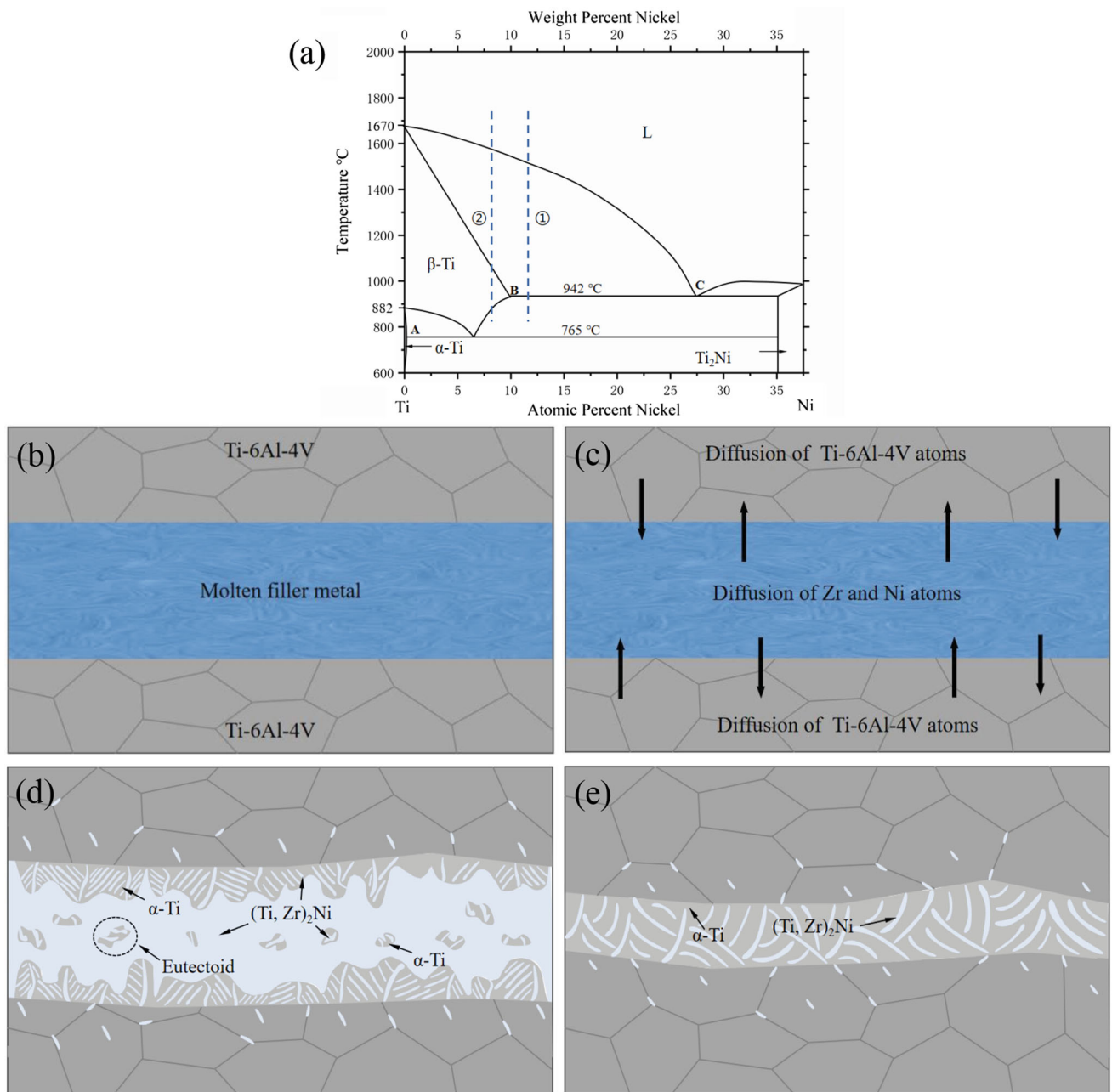


Fig. 10 The Ti(Zr)–Ni phase diagram and a conceptual interface evolution model: (a) schematic phase diagram of Ti(Zr)–Ni, (b)–(e) conceptual interface evolution model of Ti–Zr–Ni brazing

5. Conclusion

Ti–38Zr–24Ni filler metal was self-designed and made. The microstructure and shear strength of the joint were investigated with variable brazing clearances. The fractured mode was also studied. Particularly, the microstructural evolution mechanism of reaction phase was thoroughly discussed. The following are our conclusions:

- (1) TC4/TC4 joint consisted of two zones with narrow brazing clearance and contained three zones with large brazing clearance. The brazing clearance (0 μm) had no center zone. Diffusion zone consisted of eutectoid structures: $\alpha\text{-Ti}$ and $(\text{Ti,Zr})_2\text{Ni}$ and remained based metal.

Interface zone was composed of eutectoid structure: $(\text{Ti,Zr})_2\text{Ni}$ and $\alpha\text{-Ti}$. Center zone was comprised of big block brittle $(\text{Ti,Zr})_2\text{Ni}$ intermetallic compounds (IMCs) and amounts of big block and tiny eutectoid structure: $(\text{Ti,Zr})_2\text{Ni}$ and $\alpha\text{-Ti}$. Increasing the brazing clearances would increase the width of center zone.

- (2) The highest shear strength of the brazed joint was 872 MPa at 0 μm under 930 $^\circ\text{C}/10$ min, which can reach 90% of the based metal. The shear strength decreased with increasing brazing clearance due to the increasing of brittle IMCs in the center zone.
- (3) The fracture of the joint with large brazing clearance took place in the central brazing seam due to the existence of brittle $(\text{Ti,Zr})_2\text{Ni}$ intermetallic compounds. The

cracks tended to generate and propagate in the bulk (Ti,Zr)₂Ni IMCs, but may be hindered by the ductile α -Ti. The fracture surface expressed two different fracture patterns: quasi-cleavage and cleavage. However, with narrow brazing clearance, the fracture occurred in the interface zone and its fracture patterns was quasi-cleavage fracture due to the disappearance of center zone.

References

1. C. Veiga, J.P. Davim and A.J.R. Loureiro, Properties and Applications of Titanium Alloys: A Brief Review, *Rev. Mater. Sci.*, 2012, **32**, p 133–148.
2. O. Botstein and A. Rabinkin, Brazing of Titanium-Based Alloys with Amorphous 25wt.%Ti–25wt.%Zr–50wt.%Cu Filler Metal, *Mater. Sci. Eng. A.*, 1994, **188**, p 305–315.
3. Y.J. Jing, H.P. Xiong, Y.L. Shang, J.S. Wang, Y.Y. Cheng and J. Jiang, Design Ti–Zr–Cu–Ni Filler Materials for Vacuum Brazing TA15 alloy, *J. Manuf. Process.*, 2020, **53**, p 328–335.
4. P. He, Z.R. Li, L. Shen and G.J. Feng, Self-Propagating Synthesis Joining of Cf/Al Composites and TC4 Alloy Using AgCu Filler with Ni–Al–Zr Interlayer, *Rare Met.*, 2021, **40**, p 1817–1824.
5. Y. Peng, J.L. Li, Y.J. Du and J.T. Xiong, Microstructure and Mechanical Properties of Joints Prepared by Vacuum Brazing on TC4 Titanium Alloy with Ag as Filler Metal, *Vacuum*, 2021, **187**, p 110134.
6. Z.W. Xu and Z.W. Li, Formation of TiAl₃ and its Reinforcing Effect in TA15 Alloy Joint Ultrasonically Brazed with Pure Al, *J. Alloys. Compd.*, 2020, **815**, p 152493.
7. S.L. Liu, J.K. Miao, W.W. Zhang and R. Wei, Interfacial Microstructure and Shear Strength of TC4 Alloy Joints Vacuum Brazed with Ti–Zr–Ni–Cu Filler Metal, *Mater. Sci. Eng. A.*, 2020, **775**, p 138990.
8. H.H. Zhang, Z.D. Cui and S.L. Zhu, Microstructure and Mechanical Properties of TC4 Joints Brazed with Ti–Zr–Cu–Sn Amorphous Filler Alloy, *Rare Met.*, 2021, **40**, p 1881–1889.
9. O. Botstein and A. Rabinkin, Induction Brazing of Ti–6Al–4V Alloy with Amorphous 25Ti–25Zr–50Cu Brazing Filler Metal, *Mater. Sci. Eng. A.*, 1996, **206**, p 14–23.
10. C.T. Chang, R.K. Shiue and C.S. Chang, Microstructural Evolution of Infrared Brazed Ti–15–3 Alloy Using Ti–15Cu–15Ni and Ti–15Cu–25Ni Fillers, *Scripta Mater.*, 2006, **54**, p 853–858.
11. C.T. Chang, Y.C. Du and R.K. Shiue, Infrared Brazing of High-Strength Titanium Alloys by Ti–15Cu–15Ni and Ti–15Cu–25Ni Filler Foils, *Mater. Sci. Eng. A.*, 2006, **420**, p 155–164.
12. D. Dong and D.D. Zhu, Brazing TiC/Ti Matrix Composite using Ti–Ni Eutectic Braze Alloy, *Vacuum*, 2018, **156**, p 411–418.
13. V.N. Radzievskii, Y.F. Gartsunov and G.G. Tkachenko, High-Temperature Brazing of Dissimilar Materials with a Wide Brazing Gap using a Filler, *Weld. Int.*, 1999, **13**, p 245–248.
14. Z.J. Chen, W. Ming and L.L. Feng, Effect of Brazing Clearance on Microstructure and Strength of Welded Joint of 316L Stainless Steel, *Adv Mater. Res. Switz.*, 2012, **399–401**, p 1890–1893.
15. P.L. Kavishe and T.J. Baker, Influence of Joint Gap Width on Strength and Fracture Toughness of Copper Brazed Steels, *Mater. Sci. Tech. Ser.*, 1990, **6**, p 176–181.
16. A. Jöckel, J. Baumgartner, W. Tillmann, J. Bültena, K. Bobzin, Influence of Brazing Process and Gap Size on the Fatigue Strength of Shear and Peel Specimen, *Welding in the world*, 2022, **150**
17. M.K. Lee and J.G. Lee, Mechanical and Corrosion Properties of Ti–6Al–4V Alloy Joints Brazed with a Low-Melting-Point 62.7Zr–11.0Ti–13.2Cu–9.8Ni–3.3Be Amorphous Filler Metal, *Mater. Char.*, 2013, **81**, p 19–27.
18. L. Li, X.Q. Li and M. Hu, Effects of Brazing Temperature and Testing Temperature on the Microstructure and Shear Strength of γ -TiAl Joints, *Mater. Sci. Eng. A.*, 2015, **634**, p 91–98.
19. I.T. Hong and C.H. Koo, Microstructural Evolution and Shear Strength of Brazing C103 and Ti–6Al–4V using Ti–20Cu–20Ni–20Zr (wt.%) Filler Metal, *Int. J. Refract. Met. H.*, 2006, **24**, p 247–252.
20. E. Ganjeh, H. Sarkhosh, M.E. Bajgholi, H. Khorsand and M. Ghaffari, Increasing Ti–6Al–4V Brazed Joint Strength Equal to the Base Metal by Ti and Zr Amorphous Filler Alloys, *Mater. Char.*, 2012, **71**, p 31–40.
21. Y.S. Cai, R.C. Liu, Z.W. Zhu, Y.Y. Cui and R. Yang, Effect of Brazing Temperature and Brazing Time on the Microstructure and Tensile Strength of TiAl-Based Alloy Joints with Ti–Zr–Cu–Ni Amorphous Alloy as Filler Metal, *Intermetallics*, 2017, **91**, p 35–44.
22. X.Q. Li, L. Li, K. Hu and S.G. Qu, Vacuum Brazing of TiAl-Based Intermetallics with Ti–Zr–Cu–Ni–Co Amorphous Alloy as Filler Metal, *Intermetallics*, 2015, **57**, p 7–16.
23. H. Donthula, B. Vishwanadh and T. Alam, Morphological Evolution of Transformation Products and Eutectoid Transformation(s) in a Hyper-Eutectoid Ti–12 at% Cu alloy, *Acta. Mater.*, 2019, **168**, p 63–75.

Publisher's Note Springer Nature remains neutral with regard to jurisdictional claims in published maps and institutional affiliations.